Role of Competitive PEO−Water and Water−Water Hydrogen Bonding in Aqueous Solution PEO Behavior

Elena E. Dormidontova

Department of Chemical Engineering and Materials Science, University of Minnesota, Minneapolis, Minnesota 55455

Received May 8, 2001; Revised Manuscript Received October 25, 2001

ABSTRACT: The behavior of aqueous solutions of poly(ethylene oxide) (PEO) is studied theoretically by applying a mean field-like approach which includes the effect of the competition of PEO and water as proton acceptors in hydrogen bond formation. Accounting for this effect is of crucial importance for a correct description of all solution properties. We calculate the temperature and concentration dependence of the average fraction of hydrogen bonds between PEO and water and find very good agreement between our predictions and experimental or MD simulation data. We also make predictions concerning the temperature behavior of the second virial coefficient A_2 and the effective interaction parameter χ_{eff} and compare it with experimental data. We found that the decrease of A_2 with temperature is caused by the delicate balance of the opposing effects of water−PEO and water−water hydrogen bonding. The phase diagram for PEO of different molecular weights in water is calculated using experimentally reported data for the energy and entropy of association. We achieved very good quantitative agreement with most of the experimental data reported, in particular reproducing the closed loop regions of phase coexistence. We also compare our findings with results of other theoretical models.

Introduction

Aqueous solutions of poly(ethylene oxide) have attracted much attention during recent decades.[1−25] On one hand this interest is due to the fascinating behavior of this polymer.[1−26] In contrast to normal polymer behavior in which the solubility increases with temperature, the solubility of PEO decreases and phase separation occurs above a critical temperature that depends on the molecular weight.[1−6] At even higher temperatures the homogeneous state becomes stable again. Thus, formation of closed loop regions of phase coexistence is one of the characteristic features of the behavior of aqueous solutions of PEO.[1−4,13−15,17,18] Such behavior is typical for polymer systems that exhibit hydrogen bonding.[27−29] As it was well understood both experimentally and theoretically, hydrogen bonding (hb) taking place in aqueous solutions of PEO is of key importance for understanding the behavior of PEO in water.[3,4,14,18−25,30]

Besides purely academic interest in the unusual behavior of this polymer, PEO has also attracted attention because of its practical importance.[31−35] PEO is biocompatible and inhibits protein adsorption.[31,32] These specific features makes polymeric micelles with a PEO corona, PEO gels and other aggregates of PEO good candidates for drug delivery purposes.[32−34] The other application of PEO is biomimetics: since PEO is biocompatible, it can replace some biopolymers and provides an insight to their behavior and functions.[36] This also has potential for biomedical use in future.

Thus it is evident that the understanding of the behavior of poly(ethylene oxide) in aqueous solutions is very desirable. A large body of experimental data has been collected for decades.[1−11,19−24] However, it is necessary to note that the extensive volume of data does not automatically ensure considerable progress in understanding. PEO is not a simple polymer to work with. It is biocompatible,[31−34,36] and it is capable of specific interactions with biomolecules which may lead to a considerable divergence of the results from different groups.[6,7,31] Also as we discussed above, PEO possesses different unusual properties and this variety of properties is due to several different interactions taking place at the same time. The result may not necessary be straightforward.

The unusual behavior of PEO in aqueous solutions has also attracted the attention of theorists[12−18] drawn by the challenge to describe these properties and, more importantly, to provide an insight to the origins of this behavior, which makes possible predictions of phenomena which have not been observed so far.

Theoretical considerations by Kjellander and Florin[12] have taken into account structural changes upon the formation of a hydrogen-bonded complex between PEO and water. The interaction between polymer monomers and with water were accounted for by considering the packing conditions for nearest neighbors with nondirectional interactions in the limit of very dilute solutions. This simple model allowed to predict the heat of dilution and partial molar entropies (enthalpies) of water with a good degree of accuracy.

One of the first attempts to predict the phase behavior of aqueous solutions of PEO was initiated by Karlström in 1984.[13] Effectively the PEO chain was replaced by a heteropolymer with a temperature-dependent number of monomers of two sorts, denoted as low- and high-temperature states of a PEO unit. These two monomers can interact with themselves, with each other and with solvent, so there are four χ parameters plus a variable ratio between the number of realizations of the low- and high temperature states.[13] Using these five variables as adjustable parameters, predictions for the phase diagram were made[13] and compared with Saeki's experimental data.[3] Although the lower critical solution temperature, (LCST) was relatively close to the experimentally reported data, the corresponding UCST was too high. Also, the closed loop region had a vertical rather than horizontal orientation, and its center was shifted to larger polymer concentration than the experimental results.[13]

10.1021/ma010804e CCC: $22.00
Published on Web 12/21/2001

Karlström's approach was generalized by Linse and co-workers using a self-consistent mean field calculations (SCMFC).[15,37,38] The methodology of the approach remains the same, considering polar and nonpolar states (the analogy of low- and high-temperature states) for PEO units and considering all possible interactions between different and similar states. The approach was extensively applied to systems containing PEO, PPO, and water, so there are at least 10 independent χ parameters.[15,37,38] Usually the values of the parameters were obtained by fitting the experimental phase diagrams. Similar to Karlström's result, comparison with the experimental data of Saeki for PEO in water[3] gives a smaller LCST for high molecular weight samples and vertically oriented loops with a UCST that is up to 50 deg higher than reported for the low molecular weight samples.[15] Although this approach does allow one to make some predictions concerning the phase behavior of aqueous solutions of PEO, it has evident disadvantages. First, it does not disclose the physical origin of the specific temperature-dependent interactions between PEO and water (hydrogen bonding), replacing them by interactions between a temperature-dependent population of polar and nonpolar monomers of an imaginary heteropolymer. Second, the multiple interaction parameters between the units of a heteropolymer and water can be found only by fitting the phase diagram.[15,37,38] If there is no experimental phase behavior data for a given polymer system, the approach cannot make even qualitative predictions about its behavior.

Another theoretical model treated hydrogen-bonded polymer mixtures (solutions) has been suggested by Prange et al.[30] They employed an oriented quasichemical approximation method to account for nonrandom mixing of polymers with hydrogen bonding sites. While in principle this approach is able to account for orientational specificity of hydrogen bonding, formation of hydrogen bonding pairs has been considered in a purely statistical way. For instance, for water among possible (10) interaction sites two were counted for donors and two for acceptors, with the remaining sites reserved for with dispersion force interactions.[30] A similar assumption was made for PEO having two acceptor sites among the 10 possible. The advantage of this model is that it attempted to account for the formation of hydrogen bonds between water molecules and between PEO and water schematically shown in Figure 1. However, upon formation of hydrogen bonds the orientation of donors and acceptors sites with respect to each other was not accounted for.[30] In addition the size of monomer units for PEO and water was assumed to be the same. For comparison with experimental data for PEO in water, −884 K was used for the energy (in units of Boltzman's coefficient) for hydrogen bonding between PEO and water, which is about 2.2 times smaller than experimentally reported (see below) and 4 times larger compared with that used for water−water association, −200 K. The latter is nearly 10 times smaller than experimentally reported data, as we will see below. Two more dispersion force interaction energies were used as a parameters of the model. The phase diagram obtained for PEO in water (and other systems of associated polymers) was qualitatively similar to experimental observations. However, quantitatively the critical points were as much as 30 deg lower than experiment.[30] To fit the critical point data a correcting factor with three additional variables was used. Thus, seven adjustable parameters were used in total in the model to predict the phase behavior for PEO in water.[30]

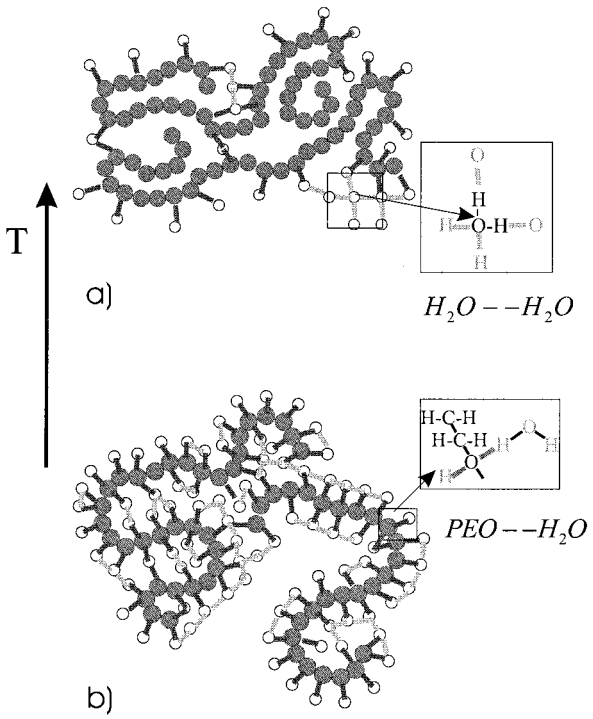

Figure 1. Schematic presentation of hydrogen bonding between water and PEO, including water−water hydrogen bonds and the corresponding chain conformation of poly(ethylene oxide) (PEO) in aqueous solutions at high (a) and low (b) temperatures.

The scaling "*p*-cluster model" by de Gennes[16] just assumes that formation of aggregates containing *p* polymer chains is favorable due to some reason and postulates a negative contribution from the *p*th order term of the free energy expansion. The coefficient before this term, ρ, and number of chains forming a cluster remain unknown parameters of the model.[16]

A purely phenomenological approach was employed by Bae et al.[17] to rationalize their experimental data for the phase behavior of aqueous solutions of PEO.[4] These authors assume an adjustable χ parameter of the form: $\chi(T,\Phi) = D(T)B(\Phi)$ where $D(T) = d_o + d_1/T + d_2 \ln T$ and $B(\Phi) = 1/(1 - b\Phi)$. The fitting of the experimental data was rather successful, but for each of the three data sets a different set of the four parameters (d_o, d_1, d_2, and b) was required. The absolute values of the parameters were rather large (see the Phase Diagram section for details), and the χ parameters predicted using the same set of adjustable parameters as for phase diagram disagree with experimental observations.[17]

The theoretical approach by Matsuyama and Tanaka[14] provides a more physical picture of aqueous solutions of PEO by accounting for the hydrogen bonding between PEO and water. They made predictions concerning the temperature dependence of the free solvent fraction and the second virial coefficient.[14] They also calculated phase diagrams for different values of parameters and achieved a fairly good agreement with the experimental data of Saeki.[3] This approach has advantages in that it uses the energy and entropy of hydrogen bonding directly and the meaning of the most of the parameters is transparent. However, it also has some

important limitations, making the results and the method less acceptable. First, although it accounted for the hydrogen bonding between PEO and water, the hydrogen bonding between water molecules has been neglected.[14] As we will see below, these two reversible associations have comparable energies per hydrogen bond formation and moreover, they compete with each other for proton donors. As a result of this limitation, this approach could not predict even some quantitative features of the behavior of aqueous solutions of PEO, as we will see below. It was assumed that only one hydrogen bond can be formed between a water molecule and PEO monomer unit,[14] and the values of the energy and entropy of hydrogen bonding (as well as the Θ temperature that corresponds to the nonassociated monomer interactions) were treated as adjustable parameters whose absolute values were often unrealistic (see Phase Diagram section for details).

A modification of Tanaka's model[14] that takes into account pressure effects has been suggested by Pincus et al.[18] They used all the assumptions of the original model[14] (i.e., no hydrogen bonding between water molecules, one hydrogen bond per monomer unit of PEO, and so on) and made an additional simplification. Instead of considering an ensemble of PEO chains with different number of hydrogen-bonded water molecules, they assumed all chains to be identical, all having exactly the average number of hydrogen bonds, $\langle X \rangle$.[18] We note that this assumption may be costly when the chains are short or the degree of association is not so large, which is the case for the temperatures where the phase coexistence for aqueous solutions of PEO occurs. They also introduced the phenomenological dependence on pressure by reducing the number of bonding sites on PEO chains under pressure. As a result this theory has four parameters, two related to energy and entropy of hydrogen bonding and the other two are the coefficients for the $\chi(T)$ dependence.[18] Using this approach in the absence of pressure they calculated the phase diagram and the dependence of the critical temperature on the chain length. A reasonably good agreement with experimental data[4] has been achieved, similar to Tanaka. In contrast to ref 14, they used more realistic (but still somewhat large) values for the energy and entropy of hydrogen bonding, but assumed that $\chi(T)$, which describes monomer interactions apart from hydrogen bonding, slightly increases with temperature.[18] So, it seems that accounting for PEO−water hydrogen bonding only is not sufficient for the model to describe the decrease of PEO solubility observed experimentally.

In the present paper we will develop a mean-field-like model that takes into account both the association between PEO and water and between water molecules themselves (schematically shown in Figure 1). One of our aims is to understand the importance of both sorts of association on the phase behavior of PEO in water. To this end it is appropriate to compare the results of our model with that of ref 14, where water−water hydrogen bonding was neglected. We will make such comparisons throughout the paper. We also intend to overcome the limitation of the previous models by accounting for the appropriate number of donor and acceptors for hydrogen bonding and by using available experimentally reported values for the energy and entropy of hydrogen bonding.

The present paper is arranged as follows. In the next section we describe our model, which can be applied for any polymer capable of hydrogen bonding with water. Then we consider the temperature and concentration dependences of the degree of association between water and PEO and between water and water. The results will be compared with experimental and computer simulation data for PEO in aqueous solutions and for pure water. In the fourth section, the temperature dependence of the second virial coefficient A_2 and χ parameter will be calculated and compared with experimental data. In the fifth section, the phase diagram for PEO in water will be obtained. The comparison with experimental data and predictions of other theories will be made. We will summarize our findings in the Conclusions.

Model

We will consider aqueous solutions of long PEO chains, i.e., the chains having $N \gg 1$ monomer units of volume v_p. Water molecules will be represented by a monomer of a volume v, which will be considered as a reference volume, i.e., a volume of a cell in the Flory−Huggins theory. The specificities of the PEO and water molecules in hydrogen bond formation will be captured via the characteristic energetic and entropic change upon hydrogen bond formation for which we will use experimentally reported data. The influence of conformational changes in PEO and water with temperature and concentration on hydrogen bond formation will be omitted here for the sake of simplicity. This factor may become important at very high temperature or high polymer concentration (where low-temperature crystallization of PEO may also take place). The conformational changes of PEO remain a complicated and controversial issue and deserve a separate analysis, which we plan to conduct in the future. It is also worthwhile to note that besides PEO−water and water−water hydrogen bonds, a hydrogen bond between the end-group hydrogen of PEO and any oxygen can be formed.[39,40] This association leads to the formation of physical network of PEO especially in the solutions with considerable PEO excess, but this effect is important mainly when the chain length is small and there is larger number of OH end groups. Hence, this sort of hydrogen bonding is of more importance for poly(ethylene glycol) compared to long PEO chains considered here. The PEO−PEO hydrogen bonding and the importance of this association for the chains of different length will be the subject of a future paper.

To obtain the free energy of the hydrogen-bonded solution, we will use the approach of Semenov and Rubinstein for solutions of associated polymers.[41] The free energy (density) of the system can be presented in the following form:

$$F = F_{ref} + F_{int} + F_{assoc} \qquad (1)$$

The free energy (per unit cell) of the reference state, a solution of noninteracting polymers, F_{ref}, has purely entropic character and is defined by

$$\frac{F_{ref}}{kT} = \frac{\Phi v}{N v_p} \ln\left(\frac{\Phi}{Ne}\right) + (1 - \Phi) \ln((1 - \Phi)/e) \qquad (2)$$

where Φ is the volume fraction of polymer.

F_{int} describes the (volume) interactions between monomers, apart from the hydrogen bonding ones:

$$\frac{F_{int}}{kT} = \chi\Phi(1-\Phi) \tag{3}$$

F_{assoc} is the part of the free energy due to PEO−water and water−water hydrogen bonding:

$$\frac{F_{assoc}}{kT} = -\frac{\nu}{V}\ln Z_{assoc} \tag{4}$$

where Z_{assoc} is the following partition function[41]

$$Z_{assoc} = P_{comb} W_p \exp\left(\frac{\Delta E_p}{kT} n_p\right) W_w \exp\left(\frac{\Delta E_w}{kT} n_w\right) \tag{5}$$

P_{comb} is the combinatorial factor describing the number of ways to form n_p hydrogen bonds between PEO and water and n_w hydrogen bonds between water molecules. ΔE_i is the energetic gain for formation a hydrogen bond between PEO and water, i = p, or between water and water, i = w. W_i is the probability that the donor and acceptor groups can be found in the vicinity of each other and with the correct orientation (with respect to each other) for formation of the corresponding hydrogen bonds. At the moment we will describe W_i in a somewhat generalized way,[41] whereas later we will assign its different parts to the particular physical effects

$$W_i = \left(\frac{v_{hb}^i}{V}\right)^{n_i} \tag{6}$$

where V is the volume of the system and v_{hb}^i is the volume per PEO−water (i = p) or water−water (i = w) hydrogen bond.

Each molecule of water carries two hydrogens which can participate in formation of hydrogen bonds either with PEO or with other water molecule (as shown schematically in Figure 1), hence the total number of proton donors for hydrogen bonds formation is $2\mathcal{N}_w$, where $\mathcal{N}_w$ is the number of water molecules. Each oxygen of PEO can participate in formation of two hydrogen bonds (see Figure 1), therefore the total number of proton acceptors on PEO chain is $2\mathcal{N}_p(N+1) \simeq 2\mathcal{N}_p N$ for long PEO chains (where $\mathcal{N}_p$ is the number of PEO chains). Similarly each oxygen of water can also accept two hydrogen bonds and the total number of proton acceptors on water is $2\mathcal{N}_w$. The number of ways to select n_p proton acceptors on PEO out of $2\mathcal{N}_p N$ total is

$$\frac{(2\mathcal{N}_p N)!}{(2\mathcal{N}_p N - n_p)! n_p!} \tag{7}$$

Similarly, the number of ways to select n_w proton acceptors on H_2O among $2\mathcal{N}_w$ total is

$$\frac{(2\mathcal{N}_w)!}{(2\mathcal{N}_w - n_w)! n_w!} \tag{8}$$

and the number of ways to select $n_p + n_w$ proton donors out of $2\mathcal{N}_w$ is

$$\frac{(2\mathcal{N}_w)!}{(2\mathcal{N}_w - n_p - n_w)!(n_p + n_w)!} \tag{9}$$

Now, to obtain the combinatorial factor we only need to take into account that the number of ways to form n_p donor−acceptor pairs between PEO and water and n_w pairs between water and water is $(n_p + n_w)!$. Therefore for the combinatorial factor we get

$$P_{comb} = \frac{(2\mathcal{N}_p N)!}{(2\mathcal{N}_p N - n_p)! n_p!}\frac{(2\mathcal{N}_w)!}{(2\mathcal{N}_w - n_w)! n_w!}\frac{(2\mathcal{N}_w)!}{(2\mathcal{N}_w - n_p - n_w)!} \tag{10}$$

Using eqs 1−6 and 10, the total free energy (per unit cell) of the polymer system can be presented in the form

$$\frac{F}{kT} = \frac{\Phi\nu}{N v_p}\ln\left(\frac{\Phi}{Ne}\right) + (1-\Phi)\ln((1-\Phi)/e) + \chi\Phi(1-\Phi) + 2\Phi\frac{\nu}{v_p}\left[x\ln x + (1-x)\ln(1-x) - x\frac{\Delta F_p}{kT}\right] + 2(1-\Phi)\left[p\ln p + (1-p)\ln(1-p) - p\frac{\Delta F_w}{kT}\right] + 2(1-\Phi)\left[\left(1-p-x\frac{\Phi\nu}{(1-\Phi)v_p}\right)\ln\left(1-p-x\frac{\Phi\nu}{(1-\Phi)v_p}\right)\right] - 2(1-\Phi)\left(p + x\frac{\Phi\nu}{(1-\Phi)v_p}\right)\ln(2(1-\Phi)/e) \tag{11}$$

Here we introduced the new variables, the average fraction of hydrogen bonds between PEO and water, x

$$x \equiv \frac{n_p}{2\mathcal{N}_p N} \tag{12}$$

and the average fraction of association in water, p

$$p \equiv \frac{n_w}{2\mathcal{N}_w} \tag{13}$$

In eq 11 we also used the relation between the number of PEO or water molecules and their volume fractions: $\mathcal{N}_p N v_p/V \equiv \Phi$; $\mathcal{N}_w \nu/V \equiv (1-\Phi)$. In addition we combined the contributions for the energetic gain and entropic loss for hydrogen bond formation in one term[28]

$$\frac{\Delta F_i}{kT} \equiv \frac{\Delta E_i}{kT} - \Delta S_i \tag{14}$$

where i = p for PEO−water and i = w for water−water hydrogen bonds and the entropic loss is defined by

$$\Delta S_i \equiv -\ln\left(\frac{v_{hb}^i}{\nu}\right) \tag{15}$$

As we have shown in our previous paper,[42] the entropic loss for formation of a hydrogen bond is connected with the loss of orientational entropy for the donor and acceptor groups which have to keep the

correct orientation inside the characteristic space angle Δ for the hydrogen bond to remain stable, i.e.

$$\Delta S = -\ln\left(\frac{1-\cos\Delta}{2}\right) \tag{16}$$

Comparing eqs 15 and 16 one can find that

$$\frac{v_{hb}^{i}}{v} = \frac{1-\cos\Delta_i}{2} \tag{17}$$

Hence, the entropic loss for formation of PEO−water and water−water hydrogen bonds can be characterized via the critical angle for the corresponding hydrogen bond formation, Δ_i.[39] The values of the characteristic angle (or entropy of association) for hydrogen bond formation can be obtained from experimental data.

Minimization of the free energy (eq 11) with respect to the average fraction of PEO−water, x, and water−water hydrogen bonding, p, leads to the following equations, respectively

$$x = \exp\left(\frac{\Delta F_p}{kT}\right)(1-x)2(1-\Phi)\left(1-p-x\frac{\Phi v}{(1-\Phi)v_p}\right) \tag{18}$$

$$p = \exp\left(\frac{\Delta F_w}{kT}\right)(1-p)2(1-\Phi)\left(1-p-x\frac{\Phi v}{(1-\Phi)v_p}\right) \tag{19}$$

These two equations are in fact "chemical-equilibrium" type of equations. Dividing one of the equations by the other yields the following connection between x and p

$$\frac{x}{p} = \exp\left[\frac{\Delta F_p - \Delta F_w}{kT}\right]\frac{(1-x)}{(1-p)} \tag{20}$$

i.e., the average fraction of PEO−water and water−water hydrogen bonds would be the same if the free energy change upon formation of each of them is equal. Equations 18−20 clearly show that these two sorts of hydrogen bonding compete with each other as they both have the hydrogens of water as a common source of proton donors. Neglecting water−water hydrogen bonding could be justified only if the corresponding free energy gain would be negligibly small compared with that for PEO−water hydrogen bonding. As we will see below, this is not the case in reality.

Temperature and Concentration Dependence of the Degree of Associations

Comparison with Pure Water. Before discussing the temperature and concentration dependences of the average degree of association between PEO and water, let us consider the limit when the fraction of polymer tends to zero, $\Phi \to 0$, and there is only hydrogen bonding in water. In this limit, eq 19 transforms into

$$p = 2\exp\left(\frac{\Delta F_w}{kT}\right)(1-p)^2 \tag{21}$$

Despite the fact that our model has a statistical character only and the different details of conformational behavior such as preferred water packing and long-range orientations are not accounted for, it should be capable of providing reasonable predictions for the average degree of association in water. To this end we need to know the energetic gain and entropic loss (or characteristic angle) for hydrogen bond formation between water molecules. The reported energy gain per hydrogen bond formation in water varies from 2.4 to 5.5 kcal/mol depending on the source of information, and whether a single or double hydrogen bond is accounted for the energy change.[39,43−50] It seems that the most widely accepted value for the energy of one hydrogen bond in water in the liquid state is 3.4 kcal/mol,[39,43,45,48] which corresponds to $\Delta E_w/k \simeq 1800$ K, and we will use this value in our calculations. As to the entropic loss per hydrogen bond formation, this value also varies widely: the corresponding characteristic angle Δ_w is in the range 10−40° for water in the liquid state.[39,43,44,48,50]

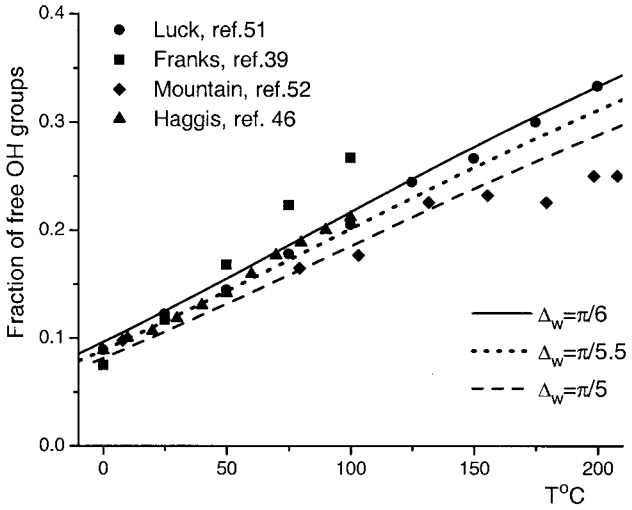

Figure 2. Temperature dependence of the average fraction of free OH group in pure water. Experimental and computer simulation data are presented as symbols: circles (ref 51); squares (ref 39, using the original results from ref 48); diamonds (ref 52, computer simulation); triangles (ref 46). Theoretical curves are the solutions of eq 21 for $\Delta E_w/k$ = 1800 K and $\Delta_w = \pi/6$ (solid curve), $\Delta_w = \pi/5.5$ (dotted curve) and $\Delta_w = \pi/5$ (dashed curve).

Different experimental techniques such as infrared and Raman spectroscopy have been employed to study hydrogen bonding in liquid water.[39,43−50] Unfortunately, often the data obtained have an ambiguous interpretation, as it is not evident whether the average fraction of hydrogen bonds measured should be assigned to the fraction of quadruple, triple, or double hydrogen bonds per water molecule or their combination.[48] Thus, among all available experimental data we selected only those that reported unambiguous values for the fraction of "broken bonds", i.e., free OH groups.[39,46,51] In Figure 2, experimental data obtained by different experimental groups and by computer simulations[39,46,51,52] are compared with the predictions of our model (eq 21) for $\Delta E_w/k$ = 1800 K and different Δ_w. In the range of temperature considered the agreement is rather good for all three curves presented, even though above 100 °C water is not in the liquid state and predictions of our model can be considered only as an extrapolation. The best agreement is achieved for $\Delta_w = \pi/5.5$, however the other two curves for $\Delta_w = \pi/6$ and $\Delta_w = \pi/5$ are also very close to the experimental data and match one or another set of experimental data. Therefore, for further calculations it seems reasonable to use Δ_w close to the values considered in Figure 2, although in some specified cases we may use somewhat smaller or larger Δ_w. In principle, the presence of PEO in solution may also have some influence on the entropy of hydrogen

bonding between water molecules, but we would not expect it to be large. Thus, it seems evident that applying realistic values for the entropy loss and energetic gain for hydrogen bond formation in pure water our simple model is capable of predicting the temperature dependence of the average fraction of hydrogen bonds (or free OH groups) in water that agrees well with experimental observations and computer simulation data. As is seen from the experimental data and our predictions, the fraction of broken bonds in the liquid water is rather low, but slightly increases with temperature.

Temperature Dependence of the Degree of Association between PEO and Water. Now let us return to the main issue of the paper: hydrogen bonding in aqueous solutions of PEO. Again, in order to make realistic predictions concerning the average fraction of hydrogen bonding between PEO and water we need to know the energetic gain per hydrogen bond. Recent measurements of NMR relaxation times show that the characteristic activation energy is about 34 kJ/mol, which is most probably corresponds to energetic gain per two hydrogen bond formation between PEO and water.[19] This leads us to the energy of $\Delta E_p/k \simeq 2000$ K per PEO−water association, which we will use for most of our further calculations. We note that this value is consistent with previously reported data,[39] and it is slightly larger than for hydrogen bonding between water molecules. Another important factor is the entropic loss for hydrogen bond formation between PEO and water. We were unable to find the corresponding experimental data (which would involve indirect measurements anyway), so we will keep Δ_p as a variable. The comparison with experimental and computer simulation data considered below has shown that Δ_p seems to be smaller than Δ_w, implying a stronger entropic restriction on hydrogen bond formation between PEO and water. This is logical enough considering that the possible arrangement of water molecules around a monomer unit of PEO is limited by the presence of neighboring units of the chain and the chain conformation in general. We note that there have been some reports on concentration dependence of the enthalpy and entropy of hydrogen bonding between PEO and water, which are likely to be associated with PEO conformational changes in the high polymer concentration range. However these results were obtained applying some questionable interpretations. We do not consider the influence of conformational effect on hydrogen bonding, and therefore, ΔE and Δ are assumed to be constant with respect to concentration throughout the paper.

Solving the set of eqs 18 and 19 numerically, one can obtain the temperature and concentration dependence of an average fraction of hydrogen bonds between PEO and water, between water molecules and the fraction of free OH groups of water. The temperature dependence of x, p, and free OH groups of water is presented in Figure 3 for $\Phi = 0.5$, $\Delta_p = \pi/8$, $\Delta_w = \pi/5$, and $v_p/v = 3$. (We will use $v_p/v = 3$ throughout the paper.) As is seen, the fraction of hydrogen bonds between PEO and water, x, and between water molecules, p, is rather large at low temperature (as shown schematically in Figure 1b) but decreases rapidly with the temperature increase (see Figure 1a) because the relative energetic gain for hydrogen bond formation decreases compared with kT. At very low temperature the degree of association between PEO and water, x, approaches that for

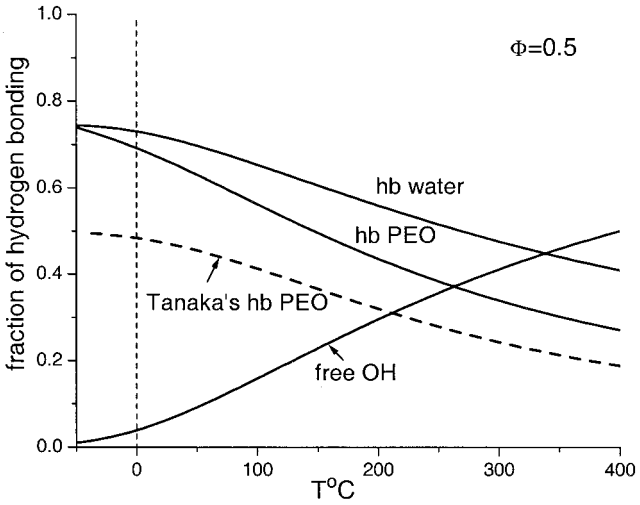

Figure 3. Temperature dependence of the average degree of hydrogen bonding (hb) between PEO and water; water and water, and the fraction of free OH groups of water. Solid curves obtained by solving eqs 18 and 19 for $\Phi = 0.5$, $\Delta E_p/k = 2000$ K, $\Delta E_w/k = 1800$ K, $\Delta_p = \pi/8$, and $\Delta_w = \pi/5$. The dashed curve represents the results of Tanaka's model[14] (see eq 23 in text) for the same set of parameters ($\Phi = 0.5$, $\Delta E_p/k = 2000$ K, $\Delta_p = \pi/8$) and $P = 2$.

water, p, due to a larger energy of association between PEO and water. However, since the entropic loss for PEO−water hydrogen bond formation was also assumed to be larger, the difference between p and x increases with temperature. The average fraction of free OH groups is very low at low temperature so nearly all water donors/acceptors are employed in association. With an increase of temperature, the fraction of free OH groups increases considerably due to the disruption of hydrogen bonds, but the degree of association between water remains rather high even at elevated temperature, in agreement with experimental observations for pure water.[39,46,51,52] The predictions of Tanaka's model[14] (which neglects water−water association) for the average fraction of PEO−water hydrogen bonds are also shown in Figure 3. As we see, Tanaka's model provides much smaller values for x compared to our results. We will discuss the physical reasons for this below when we will consider the concentration dependence of the average fraction of association.

It is worth while to note that having more general character our model can reproduce Tanaka's results in some limits. If we consider in accordance with Tanaka's assumptions[14] that (i) $p = 0$, i.e., there is no hydrogen bonding of water, and (ii) a molecule of water is capable of forming only one hydrogen bond with any oxygens of PEO, that would lead to the following transformation of eq 18

$$x = \exp\left(\frac{\Delta F_p}{kT}\right)(1-x)(1-\Phi)\left(1 - 2x\frac{\Phi v}{(1-\Phi)v_p}\right) \quad (22)$$

Assuming that parameter P in Tanaka's model (standing for the total fraction of functional group on a polymer chain with respect to the number of monomer units N) is equal to $2v/v_p$, eq 22 coincides with results of Tanaka's model.[14] We note that Tanaka assumed the volume for monomer unit of a solvent and a polymer to be the same, $v_p = v$, so that taking into account valency

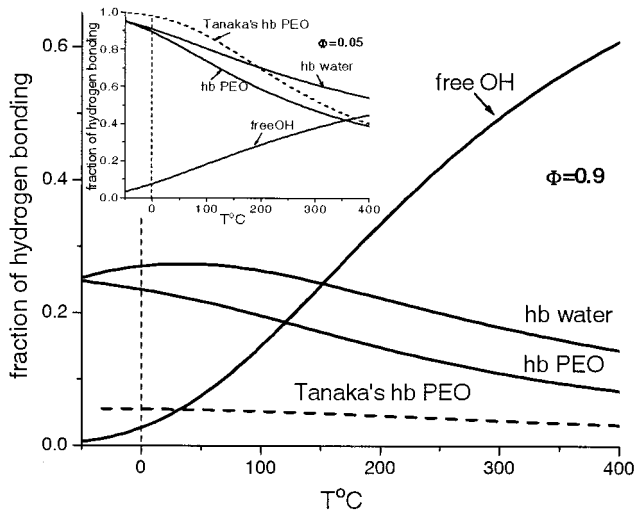

Figure 4. Temperature dependence of the average degree of hydrogen bonding (hb) between PEO and water, water and water, and the fraction of free OH groups of water. Solid curves obtained by solving eqs 18 and 19 for $\Phi = 0.9$, $\Delta E_p/k = 2000$ K, $\Delta E_w/k = 1800$ K, $\Delta_p = \pi/8$, and $\Delta_w = \pi/5$. The dashed curve represents the results of Tanaka's model[14] (see eq 23 in text) for the same set of parameters ($\Phi = 0.9$, $\Delta E_p/k = 2000$ K, $\Delta_p = \pi/8$) and $P = 2$. The insert picture is the temperature dependence of the average degree of associations and the fraction of free OH groups of water for $\Phi = 0.05$. The other parameters are the same. The results of Tanaka's model are presented as well.

of oxygens of PEO we obtain $P = 2$ for Tanaka's model of PEO in water and

$$x = \exp\left(\frac{\Delta F_p}{kT}\right)(1 - x)(1 - \Phi)\left(1 - Px\frac{\Phi}{(1 - \Phi)}\right) \quad (23)$$

We used this equation (with $P = 2$ and the same values of other parameters as employed in our model) for comparison our results with Tanaka's model in Figure 3. We note that Tanaka used $P = 1$ in all numerical calculations presented in ref 14.

For low polymer concentration, $\Phi = 0.05$ shown in the insert of Figure 4, both the average fraction of PEO−water and water−water hydrogen bonds increases (and the difference between x and p at small T decreases) compared to the case $\Phi = 0.5$ because of the larger fraction of donors/acceptors available for hydrogen bonding. Qualitatively the temperature dependence is similar to that considered above. It is interesting to note that Tanaka's model[14] predicts a larger value of hydrogen bonding between PEO and water than our model. This is in striking contrast with the data for $\Phi = 0.5$. We will return to the explanations of this effect below when the concentration dependence will be discussed. Now let us consider the opposite situation, when PEO is the dominant component of the solution, i.e., $\Phi = 0.9$ (Figure 4). In this case the fraction of hydrogen bonds in PEO and water are much smaller than that for lower polymer concentrations considered in Figures 3 and the insert. The reason is in the decrease of the number of proton donors for hydrogen bonding and proton acceptors for water−water hydrogen bonds. The temperature dependence of the average fraction of hydrogen bonds in water, p, exhibits a maximum at about 40 °C. The reason for this effect is likely to be the redistribution of hydrogen bonds between PEO and water which is especially pronounced when the fraction of proton donors for both sorts of association is small. At low temperature the energetic gain for hydrogen bond formation with PEO is large, but as the temperature increases the entropic penalty for this association becomes significant. Consequently some of the proton donors that are freed by the hydrogen bond disruption reassociate with water leading to an increase in p until some critical temperature is reached. Below this temperature reassociation with water becomes unfavorable due to its own entropic loss. Once again, the predictions of Tanaka's model for the fraction of PEO−water hydrogen bonding[14] are smaller than in our model.

Comparison with Experiment. Experimentally the value which can be extracted from the measurements, the so-called hydration number, is a complex characteristic of hydrogen-bonded water surrounding PEO. For instance, the hydration number can be considered as the number of water molecules which can be packed on the surface of a PEO monomer.[24] Depending on the experimental technique applied and the range of concentrations studied the hydration number can vary from 1 to 6 water molecules per PEO unit at fixed temperature.[11,20−24] Most experiments are for approximately equal weight fractions of polymer and water.[20−22] For this case the hydration number contains both the fraction of water directly hydrogen-bonded to PEO, N_{hb}^{exp} and water bound to PEO indirectly, i.e., via intermediate water molecule(s) directly (hydrogen) bonded to PEO, N_w^{exp}. N_{hb}^{exp} can be compared with the $2x$ value in our predictions, assuming that each hydrogen bond formed between PEO and water implies another water molecule hydrogen bonded with PEO. This seems to be a reasonable assumption for the case of dilute and semidilute solutions where there is no lack of water. In contrast to N_{hb}^{exp}, the fraction of indirectly bound water, N_w^{exp} can be hardly estimated theoretically as the experimentally reported value for hydration number strongly depend on the technique applied for measurements and interpretation involved.[11,20−24]

In Figure 5, the experimentally obtained temperature dependence of the hydration number for aqueous solutions of relatively long PEO chains (with $\Phi \simeq 0.5$)[20−22] is compared with our theoretical predictions. To obtain the theoretical prediction for the hydration number we assumed that the temperature dependence of the observed hydration number is due to the change in the fraction of directly bound water, N_{hb}^{exp}, only. N_{hb}^{exp} was counted as a temperature-independent constant, which was obtained by fitting one data point at some intermediate temperature. Using this assumption we get nearly perfect match between our predictions (for $\Delta_p = \Delta_w = \pi/18$) and experimental data for PEO 2000.[22] We note that, to obtain a temperature dependence similar to that experimentally observed we had to assume a relatively small (but not unrealistic) characteristic angle for PEO−water and water−water association (i.e., a relatively large entropic loss for hydrogen bond formation). Any additional temperature dependence of the fraction of indirectly bound water, $N_{hb}^{exp}(T)$, would shift Δ_p and Δ_w to larger values, which correlates better with experimental observations.

The temperature dependence for PEO 1000 and shorter PEG chains (see insert) deviates from the nearly linear dependence observed for PEO 2000. The nonlinearity of the dependence increases with a decrease of the chain length. By choosing slightly different value for the characteristic angle for hydrogen bonding (and

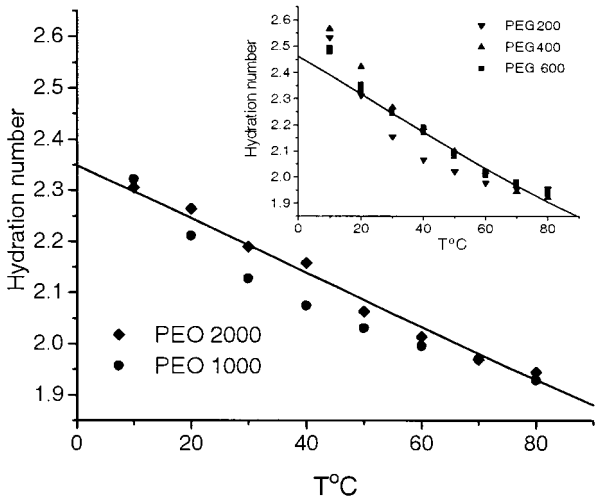

Figure 5. Temperature dependence of the hydration number for high and low molecular weight (insert) PEO in aqueous solution. Experimental data are represented by symbols: PEO 2000 ($N = 45$), ref 22 (diamonds); PEO 1000 ($N = 23$), ref 22 (circles); PEG 600 ($N = 13$), refs 20−22 (squares); PEG 400 ($N = 9$), ref 22 (up triangles); PEG 200 ($N = 5$), ref 22 (down triangles). Theoretical dependences were calculated for $\Phi = 0.5$ (corresponding to experimental conditions), $\Delta E_w/k = 1800$ K, assuming that the variation in hydration number is due to changing the fraction of hydrogen bonded with PEO water molecules ($2x$ in our model, from eq 18). The fraction of indirectly bound water contributing to hydration number was taken to be a constant, C. The value of the constant was obtained by fitting experimental data for $T = 30$ °C. For the main plot, we used $\Delta E_p/k = 2000$ K, $\Delta_p = \Delta_w = \pi/18$, and $C = 0.92$; for the insert plot, we used $\Delta E_p/k = 2100$ K, $\Delta_p = \Delta_w = \pi/30$, and $C = 1.1$.

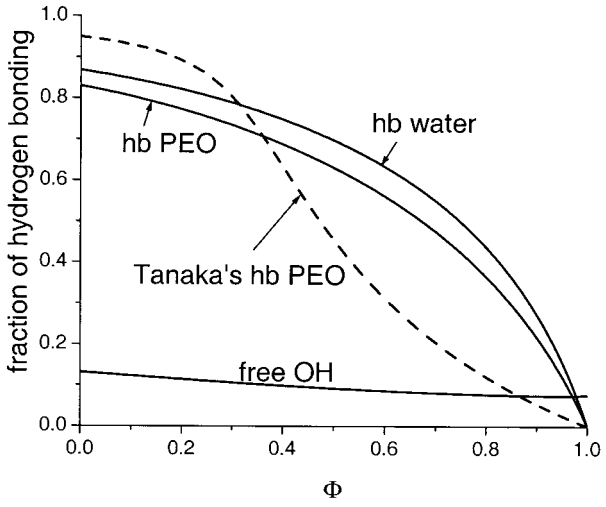

Figure 6. Concentration dependence of the average degree of hydrogen bonding (hb) between PEO and water, water and water, and the fraction of free OH groups of water. Solid curves obtained by solving eqs 18 and 19 for $T = 50$ °C, $\Delta E_p/k = 2000$ K, $\Delta E_w/k = 1800$ K, $\Delta_p = \pi/8$, and $\Delta_w = \pi/5$. Dashed curve is the results of Tanaka's model[14] for the same set of parameters ($T = 50$ °C, $\Delta E_p/k = 2000$ K, $\Delta_p = \pi/8$) and $P = 2$.

somewhat larger energy for PEO−water hydrogen bonding), we also can get reasonable agreement between our predictions and the temperature dependence of the hydration number for shorter PEG chains[20−22] for temperatures higher than 20 °C (see insert). The deviations between our predictions and experimental observations for a low temperature or very short chains (PEG 200) is most probably due to the "ends effect". As we discussed above, PEO is capable of forming hydrogen bonds with each other or water by means of OH end group. This effect is neglected in the present model as the fraction of such groups is negligibly small for long PEO chains. However for the short ones, their fraction is comparable with a total fraction of oxygens on PEO and as a result end effect can contribute to the temperature dependence especially at low temperature, where the degree of association tends to be the maximum one.

Concentration Dependence. The concentration dependence of the average fraction of hydrogen bonding between PEO and water, x, between water molecules, p and the fraction of free OH groups is shown in Figure 6 for the fixed temperature, $T = 50$ °C. Both x and p decrease with an increase of PEO content in agreement with our observations for temperature dependences considered in Figures 3 and 4. In the whole range of concentrations the fraction of PEO−water hydrogen bonds remains lower than that for water−water hydrogen boding (for the set of characteristic angles for both hydrogen bonding employed: $\Delta_p = \pi/8$, $\Delta_w = \pi/5$). The difference in association rates, $p - x$, approaches a maximum at $\Phi \simeq 0.7$ and decreases considerably as $\Phi \rightarrow 1$. The fraction of free OH groups of water is slightly decreases with polymer concentration remaining at very low (relative to x, p) level in the whole concentration range. Comparing our $x(\Phi)$ dependence with predictions of the Tanaka model,[14] to study the effect of water−water association, one can note that even qualitatively the dependencies are different. In our case, the dependence has a convex shape in the whole range of Φ, whereas Tanaka's model provide a convex shape of the curve for the region of the dominance of water and a concave shape for PEO-rich region. Accordingly Tanaka's prediction for the fraction of hydrogen bonding between PEO and water exceeds our predictions for small Φ ($\Phi \leq 0.3$ for the case of Figure 6), and it is considerably smaller than our x for the rest of concentration range. Intuitively one might expect that since Tanaka's model[14] does not take into account hydrogen bonding between water, i.e., there is no competition for proton donors, then the degree of association should be larger for his model (compared to our x) over the whole concentration range. However, one should also take into account that since there is no hydrogen bonds between water in Tanaka's model, then there is not a "network of water" and each water molecule represents a separate moiety. As a result each water molecule loses considerable translational entropy upon hydrogen bonding with PEO (especially in the region of not-so-large water content), which decreases the fraction of hydrogen bonds between PEO and water in Tanaka's model in PEO-rich region. Our approach does not have this limitation as we consider a more realistic picture of hydrogen-bonded water. Because very little "free water" is present in this region there is "nothing to lose" for a water molecule: it only has a choice of being hydrogen-bonded with PEO or with other water molecules. This explains also the difference in the results of the present model and Tanaka's theory for the temperature dependence of the average degree of association between PEO and water considered above (Figures 3 and 4).

Comparison with Computer Simulations. It is worth while to compare our predictions for the concentration dependence of the degrees of association with the recent data of molecular dynamics (MD) simulations

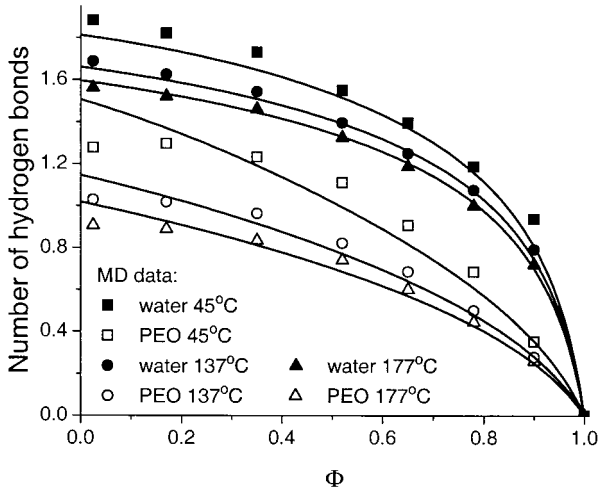

Figure 7. Concentration dependence of the average number of hydrogen bonds between PEO and water and between water molecules. Molecular dynamic (MD) simulation data from ref 25 are presented as symbols: squares (T = 45 °C); circles (T = 137 °C); triangles (T = 177 °C). Data corresponding to PEO−water association are shown as open symbols and those for water−water association as solid symbols. Results of our model are presented as solid curves. All curves are obtained using the same set of parameters, $\Delta E_p/k$ = 2000 K, $\Delta E_w/k$ = 1800 K, $\Delta_p = \pi/9$, and $\Delta_w = \pi/3.6$, for T = 45, 137, and 177 °C.

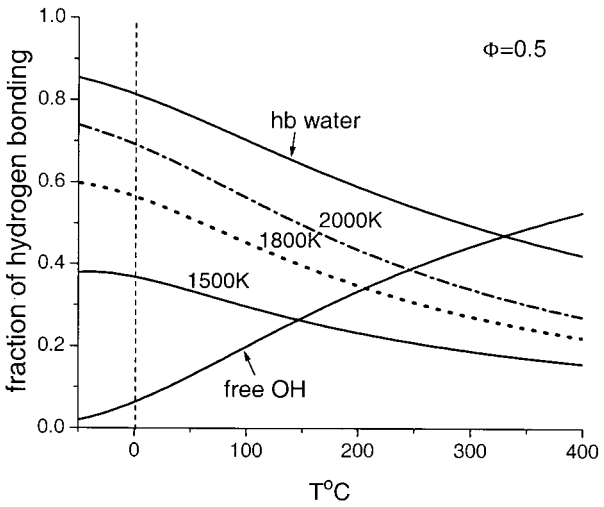

Figure 8. Temperature dependence of the average degree of hydrogen bonding (hb) between the (less soluble than PEO) polymers and water. The average fraction of water−water association and the fraction of free OH groups of water are shown only for $\Delta E_p/k$ = 1500 K since the change of the corresponding values with a decrease in ΔE_p is within a few percent. The curves are obtained by solving eqs 18 and 19 for Φ = 0.5, $\Delta E_w/k$ = 1800 K, $\Delta_p = \pi/8$, $\Delta_w = \pi/5$, and $\Delta E_p/k$ = 2000 K (dashed curve), $\Delta E_p/k$ = 1800 K (dotted curve), and $\Delta E_p/k$ = 1500 K (solid curves).

of aqueous solutions of polyoxyethylene: H−[−CH_2−O−CH_2−]$_{12}$−H.[25] Both polymer−water and water−water hydrogen bonding was counted in the simulations. We note that the polymer considered has no OH groups at the end, so that the "ends effect" were absent, similar to assumptions of our model for long PEO chains. The results of the computer simulations[25] for the number of hydrogen bonds between PEO and water and between water molecules are presented for three different temperatures in Figure 7 together with the predictions of our model. As is evident from comparison of Figures 6 and 7, our expectations for the concentration dependence of the degree of association (discussed above) are qualitatively similar to MD simulations results with all theoretical curves and experimental dependencies having convex shape. According to MD simulations the fraction of hydrogen bonding between water considerably exceeds that between PEO and water. This result can be due either to the smaller interaction energy for PEO−water binding (compared to the experimental observations and estimations of dimethoxyethane−water dimer binding energy from quantum chemistry) or to a stronger entropic loss for PEO−water association (compared to that for water i.e., $\Delta_p \ll \Delta_w$) under the conditions of the computer simulations. Since the latter is likely to be the case, we also will assume the critical angle of PEO−water association to be considerably smaller than that for water. Applying $\Delta_p = \pi/9$ and $\Delta_w = \pi/3.6$ and using the standard set for the energies of association for all three temperatures, we obtain the results shown in Figure 7 as solid curves. The agreement achieved between the theoretical and computer simulations data is remarkably good, especially for the two higher temperatures. For 45 °C, there is some deviation from the curve for the fraction of PEO−water association, as our model predicts somewhat higher degrees of association in the low concentration range. However, since the uncertainty range for the MD results has not been shown in ref 25, it is possible that the deviations of our prediction from the MD calculation lie well inside the uncertainty range. If we achieve better agreement between our predictions and MD results for this temperature, then the agreement for the other two temperatures becomes worse. It is possible that the interaction potentials used for the MD simulation reflect the temperature changes in somewhat different way than in the present model. This would be especially important for the significant temperature difference between 45 °C and the other two temperatures.

Temperature Dependence for a Different Energy of Polymer−Water Association. So far for most of the cases considered we have used fixed values for the energy and entropy of polymer/water association. As we discussed above, the present approach can be also used for prediction the behavior of other polymers capable of hydrogen bonding with water. For instance, if a polymer is characterized by a smaller energetic gain compared to PEO for hydrogen bond formation with water, e.g., ΔE_p = 1800 K and ΔE_p = 1500 K, then the temperature dependence of the degree of association will be as that shown in Figure 8. As we can see, the smaller energetic gain per polymer−water association leads to a considerable decrease in the degree of association. The degree of association between water molecules and the fraction of free OH groups increases only a few percent, so only the curves corresponding to ΔE_p = 1500 K are shown in Figure 8. Since the other parameters used for the calculation of Figure 8 are the same as that for Figure 3, the latter can be referred to for the temperature dependence of the average degree of association between water and the fraction of free OH group for ΔE_p = 2000 K. It is interesting to note that for small ΔE_p, (e.g., ΔE_p = 1500 K) the decrease in the degree of polymer−water association is less dramatic than that for water−water association (even through Δ_w is larger than Δ_p). The origin of this effect is that the competition between the polymer and water for proton donors for hydrogen bonding is rather unequal with a strong preference for water association, so little or no redis-

tribution of hydrogen bonds occurs at all. The absolute value of the average degree of polymer−water association is smaller than that for PEO (i.e., $\Delta E_p = 2000$ K). Therefore it is reasonable to expect that for such polymers the characteristic Θ temperature will be lower than that for PEO. Poly(propylene oxide) (PPO) can serve as an example of such a polymer.[1] In the ternary blends of PEO, PPO, and water or PEO−PPO di-/triblock copolymers in aqueous solutions there are several sorts of hydrogen bonding involved leading to the complex phase behavior observed.[37,38] We expect to generalize the present model to study behavior of such complex polymer systems.

Second Virial Coefficient A_2

To calculate the second virial coefficient one can consider the expansion of the osmotic pressure into the power series of the volume fraction of polymer around zero polymer concentration:

$$\Pi = \Pi_o + \left(\frac{\partial \Pi}{\partial \Phi}\right)\Big|_{\Phi=0}\Phi + \frac{1}{2}\left(\frac{\partial^2 \Pi}{\partial \Phi^2}\right)\Big|_{\Phi=0}\Phi^2 + ... \qquad (24)$$

The coefficient at the quadratic term gives us the value of the second virial coefficient:

$$A_2 = \frac{1}{2}\left(\frac{\partial^2 \Pi}{\partial \Phi^2}\right)\Big|_{\Phi=0} \qquad (25)$$

Differentiating the free energy (eq 11) with respect to polymer volume fraction and using the equations for the average degree of association between PEO and water and water−water (eqs 18−20), we obtain the (reduced) chemical potential ($\mu = dF/d\Phi$) and osmotic pressure ($\Pi = \mu\Phi - F$)

$$\frac{\mu}{kT} = \frac{v}{Nv_p}\ln\frac{\Phi}{N} - \ln(1-\Phi) + \chi(1-2\Phi) + 2\frac{v}{v_p}\ln(1-x) - 2\ln(1-p) - 2\ln\left(1 - p - x\frac{v}{v_p}\frac{\Phi}{1-\Phi}\right) \qquad (26)$$

$$\frac{\Pi}{kT} = \frac{\Phi v}{Nv_p} - \ln(1-\Phi) + 1 - \Phi - \chi\Phi^2 - 2\frac{v}{v_p}x\Phi - 2\ln(1-p) - 2p(1-\Phi) - 2\ln\left(1 - p - x\frac{v}{v_p}\frac{\Phi}{1-\Phi}\right) \qquad (27)$$

In the next section, we will use the expressions for both chemical potential and osmotic pressure to obtain the phase diagrams. Now, taking the second derivative of osmotic pressure and using eq 25, we obtain the second virial coefficient A_2:

$$A_2 = \frac{1}{2} - \chi + \frac{2}{1+p_o}\left(x_o\frac{v}{v_p} - p_o + \frac{1}{2}\frac{{x_o}^2}{(1-p_o)}\left(\frac{v}{v_p}\right)^2\right) \qquad (28)$$

We note that since the coefficient of the quadratic term in eq 24 is taken in the limit $\Phi \to 0$, the same limit should be taken in equations on x and p (eqs 18 and 19) to calculate x_o and p_o in eq 28. In the limit when there is no hydrogen bonding in the solution, i.e., $x_o \to 0$, $p_o \to 0$, the second virial coefficient assumes the usual form: $A_2 = 0.5 - \chi$. If there is no association between solvent only, $p_o \to 0$, but $x_o \neq 0$, eq 28 recovers Tanaka's prediction for A_2 (with $P = 2$). In the opposite limit, when there is no association between polymer and solvent ($x_o \to 0$), but an association of solvent is present ($p_o \neq 0$), there is still some contribution into the second virial coefficient due to that association: $A_2 = 0.5 - \chi - 2p_o/(1 + p_o)$. Since $0 < p_o \leq 1$, the second virial coefficient decreases as a consequence of the association among solvent molecules. This result is not surprising since association among one component of the blend leads to effective "demixing" from the other component, which is equivalent to an attraction among the other component. Thus, as one could expect association between PEO and water (accounted in eq 28 via terms depending on x_o) increases the second virial coefficient, i.e., leads to stabilization of solution, whereas water association (terms depending on p_o) has the opposite effect, enhancing demixing tendencies.

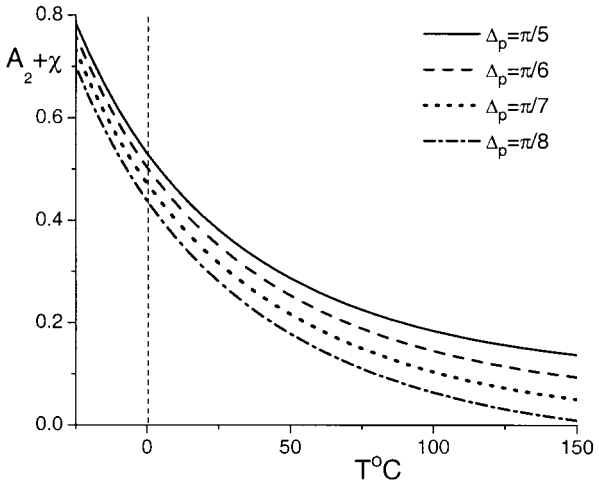

Figure 9. Temperature dependence of the hydrogen-bonding-dependent part of the second virial coefficient, $A_2 + \chi$ for the different critical angle for PEO−water association. $A_2 + \chi$ was calculated using eq 28 for $\Delta E_p/k = 2000$ K, $\Delta E_w/k = 1800$ K, and $\Delta_w = \pi/5$.

The temperature dependence of the second virial coefficient is influenced by both, the χ parameter of monomer interactions in the absence of hydrogen bonding (the second term in eq 28) and the part caused by hydrogen bonding (the third term in the equation). Let us analyze the temperature dependence of the latter term first. To this end, we plot $A_2 + \chi$ in Figure 9 as a function of temperature for different values of the characteristic angle for hydrogen bonding Δ_p (i.e., for different entropic losses for PEO−water hydrogen bonding) and fixed Δ_w ($=\pi/5$). As is seen, the part of the second virial coefficient reflecting specific interactions between PEO and water, $A_2 + \chi$, decreases strongly with an increase of temperature due to disruption of hydrogen bonds. This leads to the decrease of solubility of PEO with an increase of temperature. The rate of decrease of $A_2 + \chi$ with an increase of T is more pronounced for smaller Δ_p. The smaller is Δ_p, the stronger the temperature dependence of the degree of association (i.e., x decreases more rapidly with temperature increase) and the larger is the degree of water association, p, due to redistribution of hydrogen bonds between PEO and water. Both the decrease in x and an increase in p lead to the decrease in the second virial coefficient, which is seen in Figure 9.

Comparison with Experiment. Now let us compare predictions of our model with experimental observations. To this end we should make some assumptions concerning χ parameter for monomer interactions in the

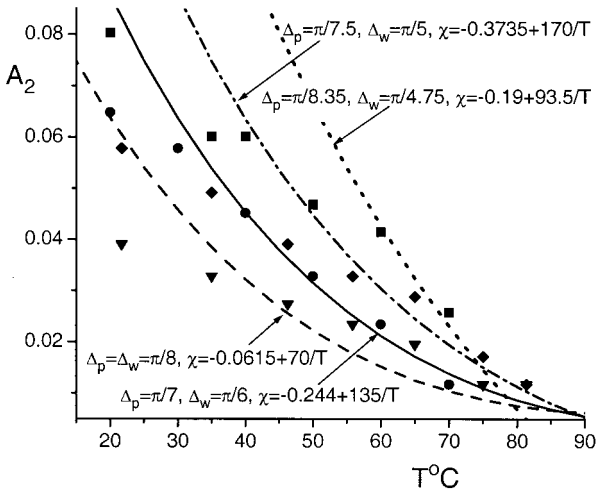

Figure 10. Temperature dependence of the second virial coefficient A_2. Experimental results are represented by symbols: PEO 13000 ($N = 295$), ref 6 (squares); PEO 16000 ($N = 364$), ref 6 (circles); PEO 11500 ($N = 261$), ref 5 (diamonds) and PEO 32800 ($N = 745$), ref 5 (triangles). Theoretical curves are calculated for $\Delta E_p/k = 2000$ K and $\Delta E_w/k = 1800$ K using different values for the critical angles and $\chi(T)$ dependences. The dotted curve is calculated for the set of parameters close to that used for the phase diagram, shown in Figure 12 (see text, Phase Diagram section).

absence of hydrogen bonding. We will assume that the temperature dependence for χ obeys the standard form

$$\chi = A + \frac{B}{T} \tag{29}$$

with B being a positive value as it is normally the case for nonassociated polymers. Naturally, there are many ways to combine some χ in the form of eq 29 with $A_2 + \chi$ (shown in Figure 9). What is evident is that the decrease in the experimentally observed[5,6] A_2 (reproduced in Figure 10 using 1.14 g/cm^3 for the PEO density[11] and 18 cm^3/mol for water molar volume to get the dimensionless value) is due to the decrease in $A_2 + \chi$ with increasing temperature as a consequence of the decrease in the degree of association between PEO and water. Depending on the values of Δ_w and Δ_p one can get a more or less strong temperature dependence for $A_2(T)$. As we discussed above, $A_2 + \chi$ changes more smoothly for $\Delta_w = \Delta_p$. Thus, using $\Delta_w = \Delta_p = \pi/8$ and $\chi = -0.0615 + 70/T$, (i.e., a rather weak $\chi(T)$ dependence) we obtained the dashed curve shown in Figure 10. Employing stronger $\chi(T)$ dependence and using larger Δ_w and Δ_p ($\Delta_p > \Delta_w$), (which ensures a more rapid decrease in A_2 with temperature increase due to hydrogen bonding) we can obtain a stronger $A_2(T)$ dependences, presented as solid and dash-and-dot curves in Figure 10. All three dependences match well with one or another set of experimental data. As is seen from Figure 10, the Θ conditions are approached for aqueous solutions of PEO in the temperature range 85−110 °C. For instance, for the set of parameters corresponding to the dash-and-dot curve the LCST of 106 °C is achieved for infinitely long polymer chains, which is comparable with experimentally observed values, discussed in the next section.

Neglecting the association of water makes the hydrogen bonding dependent part of A_2 considerably larger. For instance, for $\Delta_p = \Delta_w = \pi/5$ (and the standard values for the energies of association) $A_2 + \chi$ in Tanaka's model (where hydrogen bonding of water molecules was neglected)[14] is about 4.5 at zero temperature whereas in our case it is 0.53 for the same set of parameters. Also $A_2 + \chi$ decreases more slowly with increasing temperature in the absence of hydrogen bonding of water molecules. So, if we combine any $\chi(T)$ dependences used for calculating the curves presented in Figure 10 with the results of Tanaka's model for $A_2 + \chi$ obtained using the same set of parameters, we arrive at unrealistically large values for A_2 with the corresponding Θ temperature far above the experimentally reported values.

The experimental temperature dependence of A_2 depends on the sample.[5,6] It is necessary to note that not only the slope of the curves[5,6] but also the absolute values for A_2 (and χ_{eff}) may differ.[5−10] Some authors reported rather small values for A_2 with a weak temperature dependence;[7] however, they also observed very large aggregates of PEO chains at 60 °C with a decrease in the aggregate molecular weight at higher or lower temperatures.[7] It was suggested[6] that the results were influenced by insufficient purity of water leading to biodegradation. Due to this reason we did not include these data to Figure 10. There is no evident influence of the molecular weight on the second virial coefficient, although, some authors reported a weak decrease in A_2 with an increase of polymer molecular weight.[9,10] Our model does not predict any molecular weight dependence of A_2 which most likely to be caused by conformational or "ends-effects", which are neglected in the present approach.

Effective χ Parameter. Assuming that A_2 can be presented in the form $A_2 \equiv 0.5 - \chi_{eff}$, the effective χ parameter for PEO in water can be written in the following form

$$\chi_{eff} = \chi - \frac{2}{1+p_o}\left(x_o\frac{v}{v_p} - p_o + \frac{1}{2}\frac{x_o^2}{(1-p_o)}\left(\frac{v}{v_p}\right)^2\right) \tag{30}$$

Using the same set of parameters as for the second virial coefficient we can compare our predictions for the effective χ parameter with experimental data for long PEO chains.[5,6] The results are presented in Figure 11. Instead of a linear increase of the χ parameter with inverse temperature as expected for polymers without specific interactions, aqueous solutions of PEO exhibit the opposite tendency: a decrease in χ parameter with a decrease of temperature. It confirms that the solubility of PEO is ensured by hydrogen bonding, as clearly seen from comparison of the first and the second terms in the equation. The first term gives rise to the increase of separation tendencies with decreasing temperature as found for most polymer systems, whereas the second term, which accounts for hydrogen bonding, successfully counteracts this tendency due to the enhancement of polymer−water associations, x, and ensures an increase of solubility.

Phase Diagram

In this section, we will make predictions concerning the phase behavior of aqueous solutions of PEO and compare them with experimental data. To calculate the phase diagram, we can first define the regions of absolute instability of the homogeneous phase by analyzing the second derivative of the free energy (eq 11) on Φ. The regions where $d^2F/d\Phi^2 \le 0$ are the instability

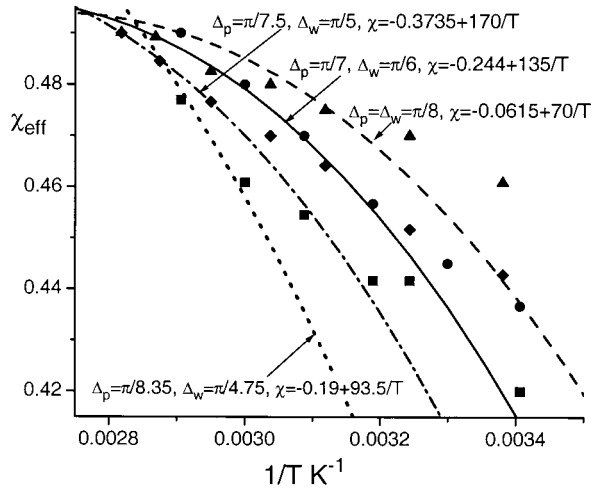

Figure 11. Temperature dependence of the effective χ parameter. Experimental results are represented by symbols: PEO 13000 ($N = 295$), ref 6 (squares); PEO 16000 ($N = 364$), ref 6 (circles); PEO 11500 ($N = 261$), ref 5 (diamonds); PEO 32800 ($N = 745$), ref 5 (triangles). Theoretical curves are calculated for $\Delta E_p/k = 2000$ K and $\Delta E_w/k = 1800$ K using different values for the critical angles and $\chi(T)$ dependences. The set of the parameters used for theoretical curves are the same as for the second virial coefficient, shown in Figure 10. The dotted curve is calculated for the set of parameters close to that used for the phase diagram, shown in Figure 12 (see text, Phase Diagram section).

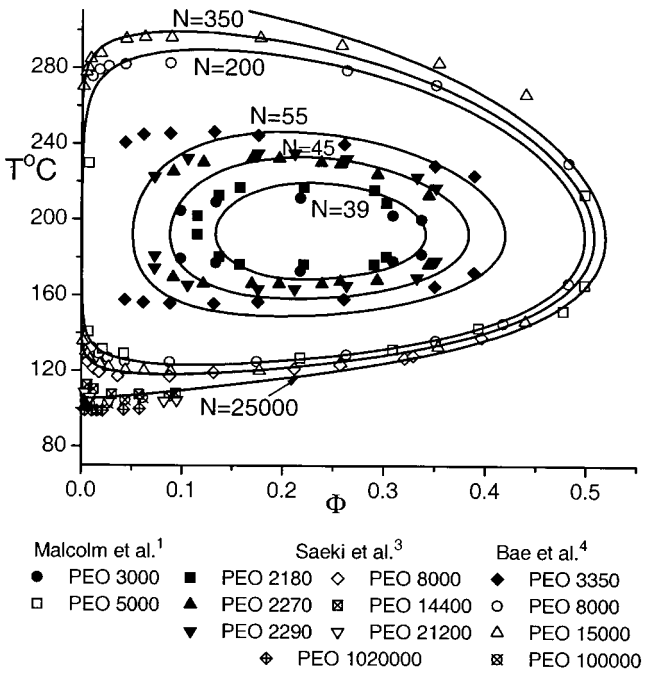

Figure 12. Phase diagram for aqueous solutions of PEO. Experimental data are represented by symbols: PEO 3000 ($N = 68$) (solid circles), PEO 5000 ($N = 114$) (open squares), Malcolm et al., ref 1; PEO 2180 ($N = 50$) (solid squares), PEO 2270 ($N = 52$) (solid up triangles), PEO 2290 ($N = 52$) (solid down triangles), PEO 8000 ($N = 182$) (open diamonds), PEO 14 400 ($N = 327$) (open squares with cross), PEO 21 200 ($N = 482$) (open down triangles), PEO 1 020 000 ($N = 23182$) (open diamonds with cross), Saeki et al., ref 3; PEO 3350 ($N = 76$) (solid diamonds), PEO 8000 ($N = 182$) (open circles), PEO 15 000 ($N = 341$) (open up triangles), PEO 100 000 ($N = 2273$) (open up circles with cross), Bae et al., ref 4. Theoretical curves are all calculated using the same set of parameters: $\Delta E_p/k = 2000$ K, $\Delta E_w/k = 1800$ K, $\Delta_p = \pi/8.35$, $\Delta_w = \pi/4.75$, and $\chi = -0.211 + 93.5/T$. The PEO polymerization number employed for calculating each of the curves is shown near the curves.

regions. Hence for the spinodal of macrophase separation we have $d^2F/d\Phi^2 = 0$:

$$\frac{v}{N\Phi v_p} - \frac{1}{1-\Phi} - 2\chi + 2\frac{(1 + xv/v_p - p)^2}{(1-\Phi)\left(1 - p^2 - x^2\frac{v}{v_p}\frac{\Phi}{1-\Phi}\right)} = 0 \quad (31)$$

It is easy to see that in the limit when where is no hydrogen bonding ($x \to 0$; $p \to 0$) eq 31 assumes the usual Flory−Huggins form for the spinodal of nonassociated polymer solution: $v/N\Phi v_p + 1/(1-\Phi) - 2\chi = 0$.

To calculate the two phase equilibrium region we can use the expressions for the chemical potential and pressure (eqs 26 and 27) we obtained before. By solving numerically the set of equations

$$\begin{cases} \mu(\Phi_1) = \mu(\Phi_2) \\ \Pi(\Phi_1) = \Pi(\Phi_2) \end{cases} \quad (32)$$

we can obtain the volume fractions of polymer in each of coexisting phases, Φ_1 and Φ_2 for fixed temperature. By varying temperature the whole space of the phase diagram can be covered.

For the phase diagram we will use the same pair of values for the energies of associations used above, $\Delta E_p/k = 2000$ K, $\Delta E_w/k = 1800$ K and the critical angle for water−water association close to that providing the best match with experimental data for pure water (Figure 2),[39,46,48,51,52] $\Delta_w = \pi/4.75$. The critical angle for PEO−water association is expected to be somewhat smaller than that for water, i.e., close to the value used before, $\Delta_p = \pi/8.35$. The values for the A and B parameters for $\chi(T)$ dependence have been chosen to get the close match with one of the experimental data. We selected the data for the intermediate molecular weight PEO, PEO 8000 ($N = 182$)[4] and get $A = -0.211$, $B = 93.5$. The results of our calculations obtained using these parameters are shown in Figure 12 as solid curves. We used the same set of parameters for all curves varying only N.

The chosen set of parameters for the phase diagram is not unique, but provides a good agreement with the set of experimental data for both high ($N = 200$, 350, ...) and low ($N = 45$) molecular weight samples. It is necessary to note that for this set of parameters the second virial coefficient turned out to be slightly larger than the experimental results presented in Figure 10. A small increase in coefficient B from eq 29 (e.g., $B = 100$ instead of $B = 93.5$) or a decrease in A (e.g., $A = 0.19$ instead of $A = 0.211$) (presented as a dotted curve in Figures 10 and 11) provides better agreement with the experimental A_2. However, in this case in order to achieve the binodals of macrophase separation that are comparable with experimental data shown in Figure 12 one has to use N values that are smaller than experimentally reported. (In general, larger values of B or smaller values of A produce wider binodal loops with a smaller LSCT and larger USCT.) The uncertainty range for the experimental phase diagram and A_2 data is unknown, and there are no measurements for the phase behavior and A_2 for the same sample in the same concentration range (and by the same group). Therefore, it is hard to conclude whether it is the limitations of

the model or the experimental uncertainty that is responsible for the slight discrepancies between (low temperature) A_2 and (high temperature) phase behavior. We also note that the theoretical A_2 (χ) is calculated in the limit of zero polymer concentration, whereas experimentally the measurements are performed for a finite concentration. It was reported that the observed concentration dependence of A_2 has a complicated form, preventing a direct extrapolation of the data to the zero-concentration limit.[6,17]

The results of different experimental groups concerning the phase behavior of PEO in aqueous solutions are also shown in Figure 12 (where we used polymer density 1.14 g/cm^3 to transform weight fractions into volume fractions).[1,3,4] The data seems to be reasonably consistent with each other even though results from different experimental groups may differ quantitatively in the values of the upper and lower critical solution temperature (UCST and LCST) for samples of similar molecular weight. For instance, UCST (LCST) for PEO 3000 ($N = 68$) studied by Malcolm et al.[1] is considerably lower (higher), ≃211 °C (≃173 °C), than the values obtained for PEO 3350 ($N = 76$) by Bae et al.,[4] ≃246 °C (≃156 °C). Also the width of the two phase region is different: ≃0.09−0.35 for the maximum width reported by Malcolm et al.[1] and ≃0.02−0.4 according to Bae et al.[4] On the other hand, the UCST and LCST for PEO 3000 ($N = 68$) studied by Malcolm et al.[1] are very close to the results of Saeki et al. for PEO 2180 ($N = 50$).[3] Similarly, higher molecular weight samples of similar molecular weight PEO 14 400 ($N = 327$)[3] and PEO 15 000 ($N = 341$)[4] provide different LCSTs, ≃107 and ≃117 °C, respectively. If the difference in molecular weight is reason for the differences pointed out above, the dependence should be reversed: a larger molecular weight yields a larger UCST and smaller LCST. It should be kept in mind that the polydispersity and possible partial thermal degradation of the samples could affect the results. It is also necessary to note that because the PEO solutions are heated in sealed Pyrex tubes,[1−4] the pressure will vary slightly with temperature. Therefore, there is some degree of uncertainty present in the reported data.

As is seen from Figure 12, there is a general agreement between the theoretical curves and experimental data.[1,3,4] The shape of the curves and the decrease in the LSCT (increase in USCT) with an increase of N are consistent with experimental observations. Also the decrease in Φ_{cr} (corresponding to the critical points) with the increase of polymer molecular weight is straightforward from both experimental observations and theoretical results. For relatively small molecular weights, even a small change in the degree of polymerization (N) results in a considerable expansion (in both temperature and composition) of the two phase coexistence region. We can compare our curve for $N = 39$ with experimental data for PEO 2180, ($N = 50$)[3] and PEO 3000, ($N = 68$).[1] Our results for $N = 45$ can be compared with that for PEO 2270, 2290 ($N = 52$)[3] and the curve for $N = 55$ with the data for PEO 3350 ($N = 76$).[4] We got reasonably good agreement between our results and experimental data for these samples even through the N values we used were slightly smaller than the experimental ones. This probably results from the molecular weight polydispersity of the experimental samples and also from the fact that we neglected any association via terminal OH groups. This association will become more important for shorter chains at larger concentrations (we intend to analyze this case in our future work). If this idea is correct, then the coexisting phase of higher concentration is effectively a gel and the region of coexistence can be broader than that for a solution.

For polymers of larger molecular weight (N), the regions of instability becomes larger and the curves corresponding to different N becomes closer to each other, converging to some limiting case. Our predictions for $N = 200$ can be compared with the experimental data for PEO 8000 ($N = 182$) by Bae et al.[4] and PEO 5000 ($N = 114$)[1] which have similar LSCT. Both the calculated LSCT and USCT are consistent with the experimental values.[4] The width of our two-phase region is only slightly narrower than the experimental data. Our curve with $N = 350$ can be compared with the data for PEO 8000 ($N = 182$) by Saeki[3] and PEO 15 000 ($N = 341$) by Bae et al.[4] Here there is also a good agreement in the values of LCST, UCST and Φ_{cr}. Our theoretical results for $N = 3000$ to 10^6 can be compared with the experimental data for PEO 14 400 ($N = 327$),[3] PEO 21 200 ($N = 482$),[3] PEO 100 000 ($N = 2273$)[4] and PEO 1 020 000 ($N = 23\,000$).[3] The LSCT (USCT) is shifted only slightly to lower (higher) T with an increase in molecular weight (N). (For example, for $N = 3000$, LSCT ≃ 108 °C, whereas for $N = 25\,000$, LSCT ≃ 106 °C). For polymer concentrations higher than Φ_{cr}, the binodal curves nearly reproduce each other for sufficiently large N (i.e., ≥3000 for our set of parameters).

It is worth while to compare the predictions of our model with results of other theoretical calculations.[13−15,17,18] The approach of Karlström[13] and later Linse with co-workers[15] provide reasonable estimates for the LCST for a low to intermediate molecular weight polymers consistent with experimental observations. However the UCST usually exceeds the experimental data by 25° (Karlström)[13] or 50° (Linse)[15] and the LCST for higher molecular weight polymers is somewhat lower than experimentally observed. There is also a qualitative difference: the closed loop region predicted theoretically has a vertical orientation in the (T, Φ) plane (in contrast to experimental horizontal one) and the center of the loop is shifted to higher Φ. Comparing our predictions with a heteropolymer model of PEO by Karlström[13] and Linse,[15] it is evident that our model provides both a better qualitative and quantitative agreement with experimental results and it does not depend on experimental phase behavior data in order to define the degree of association between PEO and water.

The phenomenological approach by Bae et al.,[17] which employs a temperature and concentration dependent χ parameter, produces a rather nice agreement with their experimental data for PEO 3350, 8000, and 15 000. However, for each molecular weight they had to use a different set of four parameters. Moreover, the absolute values of the parameters were rather large: for instance, for d_o (analogous to A in our definition of χ) they used 60 for PEO 3350, 46 for PEO 8000, and 25 for PEO 15 000, and for d_1 (analogous to B in our definition of χ) they used −3900, −3000, and −1600, respectively.[17]

The results of physically more realistic models of PEO in water by Tanaka[14] and by Pincus and coworkers[18] were also consistent with the experimental data. For these models the physical meaning of the parameters is transparent; however, the absolute

values used are often unrealistic. Thus the energy of PEO−water hydrogen bonding in Tanaka's model[14] (who used Saeki's data[3] for comparison) was about $\Delta E_p/k = 4380$ K, which is close to the largest energy for single hydrogen bonding ever reported.[53] The entropy of association was assumed to be very large; the corresponding angle ($\Delta_p < 1°$) is smaller than that for pure ice.[39] In addition the Θ temperature for monomer interactions in the absence of hydrogen bonding was 730 K, which seems to be unrealistically large. Also, the polymerization index used for predicting the closed loop region of instability was approximately five times smaller than that for the corresponding experimental samples (i.e., $N = 10-11$, theoretically, whereas experimentally $N \simeq 50-53$).[14] Pincus and co-workers[18] used more realistic values for the energy and entropy of the hydrogen bonding $\Delta E_p/k = 2400$ K, $\Delta_p \simeq 7.8°$ (even through the energy is somewhat larger than experimentally reported). However, to obtain a reasonable agreement with Bae's experimental data (for PEO 3350, 8000, and 15 000),[4] they have to use a χ parameter for interactions between monomers in the absence of hydrogen bonding that was weakly increasing with temperature: $\chi(T) = 2.88 - 0.00362/T$. Compared to the statistical models by Tanaka et al.[14] and Pincus et al.,[18] our model accounts for water−water hydrogen bonding, and we used realistic values for the energy and entropy of associations[19,39,43,45,48] (employing experimentally reported values) and $\chi(T)$ dependence for the monomer interaction energy (in the absence of hydrogen binding). In contrast to all previous studies, we did not limit the set of experimental data used for comparison to the results of one experimental group but considered the data of three independent researchers[1,3,4] with a total of 13 different PEO samples (see Figure 12). Our predictions of the phase behavior for polymers of increasing chain length are systematically consistent with experimental observations covering the whole space of experimentally reported phase diagrams.

Conclusions

We have suggested a theoretical model to describe the behavior of poly(ethylene oxide) in aqueous solutions. In contrast to the previous theories,[13−18] our model accounts for two sorts of hydrogen bonding taking place in the polymer system: PEO−water and water−water hydrogen bonding. It has been shown that this latter hydrogen bonding is of crucial importance for a correct description and understanding of the behavior of aqueous solutions of PEO. We took into account the possibility of the formation of two hydrogen bonds between a water molecule and PEO, which was also omitted in the previous models.[14,18] The influence of conformational factors on hydrogen bond formation is accounted for in our model via the characteristic energy and entropy of hydrogen bonding, without considering the precise structure of polymer and water and corresponding packing conditions. For the energy and entropy of hydrogen bonding we used values reported experimentally[19,39,43,45,48] (except for the entropy of PEO−water association, which was not found in the literature, but was expected to be only somewhat larger than that for water). The model can be used for any polymer capable of hydrogen bonding (or other reversible association) with water as long as the energy and entropy of association are known.

In the framework of our model, we calculated the temperature and concentration dependence of the average degree of association between PEO and water, between water molecules and the fraction of free OH groups of water. The results have been compared with experimental dependencies for the hydration number,[20−22] MD simulation results for H−[−CH_2−O−CH_2−]$_{12}$−H in water[25] and experimental data for pure water.[39,46,48,51,52] In all cases, we found a very good agreement. The agreement with MD simulation data[25] achieved by using the same set of parameters for three different temperatures is especially impressive since the comparison was made directly without involving any additional assumptions. To define the importance of water−water hydrogen bonding, we compared our predictions with the results of Tanaka's model (neglecting the association)[14] and found that Tanaka's model overestimates the degree of association between PEO and water at low polymer concentration and considerably underestimates this value for high polymer concentration. As a result, even the qualitative concentration dependencies predicted by the two models are different.

We also make predictions concerning the temperature dependence of the second virial coefficient, A_2 and effective χ_{eff} parameter for PEO in water. Association between PEO and water leads to an increase in A_2 (in agreement with previous results by Tanaka et al.[14]), so that the decrease in the degree of association with increasing temperature causes a decrease in A_2 as well. Water−water association is found to have the opposite effect on A_2. Combination of these two tendencies ensures a decrease in PEO solubilization followed by an increase in solubilization at elevated temperatures. We found a good agreement between the predictions of our model for both A_2 and χ_{eff} and experimental observations.

We also compare our calculated phase diagram for PEO of different chain length with experimental data reported by three different groups.[1,3,4] The agreement is especially good for long and moderate length of polymers, for which our model was originally designed. Applying the same set of parameters for shorter polymers, we obtain good agreement for some samples and somewhat less good for others. We believe that the reason for this discrepancy may originate from the molecular weight polydispersity of experimental samples and/or from the neglect of hydrogen bonding via terminal OH groups in the present approach. Association via terminal OH groups may also be responsible for strong elongation of the closed loop regions of coexistence along the Φ direction. We plan to take end effects into account in our future work. Compared to other theoretical models, our approach has the advantage of (i) accounting more completely for all the molecular interactions and the correct number of donor and acceptor groups for hydrogen bonding, (ii) employing the experimentally reported values for the energy and entropy of hydrogen bonding (as well as realistic values for $\chi(T)$ dependence), and (iii) providing physical explanations for the effects observed. The predictions of our model are more consistent with experimental results than previous theories, which we believe demonstrates the importance of the competition between the oxygens on the PEO and water as proton acceptors for hydrogen bonding.

Acknowledgment. I appreciate helpful discussions with D. Morse, T. Lodge, and M. Feldstein. This work was supported by the University of Minnesota MRSEC Program (Award DMR-9809364.)

References and Notes

(1) Malcolm, G. N.; Rowlinson, J. S. *Trans. Faraday. Soc.* **1957**, *53*, 921.
(2) Bailey, F. E.; Callard, R. W. *J. Appl. Polym. Sci.* **1959**, *1*, 56.
(3) Saeki, S.; Kuwahara, N.; Nakata, M.; Kaneko, M. *Polymer* **1976**, *17*, 685.
(4) Bae, Y. C.; Lambert, S. M.; Soane, D. S.; Prausnitz, J. M. *Macromolecules* **1991**, *24*, 4403.
(5) Strazielle, C. *Makromol. Chem.* **1968**, *119*, 50.
(6) Venohr, H.; Fraaije, V.; Strunk, H.; Borchard, W. *Eur. Polym. J.* **1998**, *34*, 732.
(7) Polik, W. F.; Burchard, W. *Macromolecules* **1983**, *16*, 978.
(8) Michalczyk, A.; Borchard, W. *Eur. Polym. J.* **1989**, *25*, 957.
(9) Devanand, K.; Selser, J. C. *Macromolecules* **1991**, *24*, 5943.
(10) Kawaguchi, S.; Imai, G.; Suzuki, J.; Miyahara, A.; Kitano, T.; Ito, K. *Polymer* **1997**, *38*, 2885.
(11) Hager, S. L.; Macrury, T. B. *J. Appl. Polym. Sci.* **1980**, *25*, 1559.
(12) Kjellander, R.; Florin, E. *J. Chem. Soc., Faraday Trans. 1* **1981**, *77*, 2053.
(13) Karlström, G. *J. Phys. Chem.* **1985**, *89*, 4962.
(14) Matsuyama, A.; Tanaka, F. *Phys. Rev. Lett.* **1990**, *65*, 341.
(15) Linse, P. *Macromolecules* **1993**, *26*, 4437
(16) de Gennes, P.-G. *C. R. Acad. Sci. Paris II* **1991**, *117*, 313.
(17) Bae, Y. C.; Shim, J. J.; Soane, D. S.; Prausnitz, J. M. *J. Appl. Polym. Sci.* **1993**, *47*, 1193.
(18) Bekiranov, S.; Bruinsma, R.; Pincus, P. *Phys. Rev. E* **1997**, *55*, 577.
(19) Lüsse S.; Arnold, K. *Macromolecules* **1996**, *29*, 4251.
(20) Maisano, G.; Majolino, D.; Migliardo, P.; Venuto, S.; Aliotta, F.; Magazú, S. *Mol. Phys.* **1993**, *78*, 421.
(21) Branca, C; Magazú, S.; Maisano, G.; Migliardo, P.; Villari, V. *J. Phys.: Condens. Matter* **1998**, *10*, 10141.
(22) Magazú, J. *Mol. Struct.* **2000**, *523*, 47.
(23) Sasahara, K.; Sakurai, M.; Nitta, K. *Colloid. Polym. Sci.* **1998**, *276*, 643.
(24) Bieze, T. W. N.; Barnes, A. C.; Huige, C. J. M.; Enderby, J. E.; Leyte, J. C. *J. Phys. Chem.* **1994**, *98*, 6568.
(25) Smith, G. D.; Bedrov, D.; Borodin, O. *Phys. Rev. Lett.* **2000**, *85*, 5583.
(26) Panayiotou, C.; Sanchez, I. C. *J. Phys. Chem.* **1991**, *95*, 10090.
(27) Walker, J. S.; Vause, C. A. *Sci. Am.* **1987**, *256*, 90.
(28) Dormidontova, E.; ten Brinke, G. *Macromolecules* **1998**, *31*, 2649; *Colloids Surf. A* **1999**, *147*, 249.
(29) Ruokolainen, J.; Makinen, R.; Torkkeli, M.; Makela, T.; Serimaa, R.; ten Brinke, G.; Ikkala, O. *Science* **1998**, *280*, 557.
(30) Prange, M. M.; Hooper, H. H.; Prausnitz, J. M. *AIChE J.* **1989**, *35*, 803.
(31) Lee, J. H.; Lee, H. B.; Andrade, J. D. *Prog. Polym. Sci.* **1995**, *20*, 1043.
(32) Allen, C.; Maysinger, D.; Eisenberg, A. *Colloids Surf. B* **1999**, *16*, 3. Kwon, G. S.; Okano, T. *Adv. Drug Delivery Rev.* **1996**, *21*, 107.
(33) La, S. B.; Okano, T.; Kataoka, K. *J. Pharm. Sci.* **1996**, *85*, 85.
(34) Riley, T.; Govender, T.; Stolnik, S.; Xiong, C. D.; Garnett, M. C.; Illum, L.; Davis, S. S. *Colloids Surf. B* **1999**, *16*, 147.
(35) Stockton, W. B.; Rubner, M. F. *Macromolecules* **1997**, *30*, 2717.
(36) Discher, B. M.; Won Y.-Y.; Ege, D. S.; Lee, J. C. M.; Bates, F. S.; Discher, D. E.; Hammer, D. A. *Science* **1999**, *284*, 1143.
(37) Malmsten, M.; Linse, P.; Zhang, K.-W. *Macromolecules* **1993**, *26*, 2905.
(38) Svensson, M.; Alexandridis, P.; Linse, P. *Macromolecules* **1999**, *32*, 637.
(39) Franks, F. *Water a Comprehensive Treatise*; Plenum: New York, 1973.
(40) Frielinghaus, H.; Pederson, W. B.; Larsen, P. S.; Almdal, K.; Mortinsen, K. *Macromolecules* **2001**, *34*, 1096.
(41) Semenov, A. N.; Rubinstein, M. *Macromolecules* **1998**, *31*, 1373.
(42) Dormidontova, E. E.; ten Brinke, G. *J. Chem. Phys.* **2000**, *113*, 4814.
(43) Scatchard, G.; Kavanagh, G. M.; Ticknor, L. B. *J. Am. Chem. Soc.* **1952**, *74*, 3715.
(44) Creswell, C. J.; Allred, A. L. *J. Am. Chem. Soc.* **1962**, *84*, 3966.
(45) Grunberg, L.; Nissan, A. H. *Trans. Faraday Soc.* **1949**, *45*, 125.
(46) Haggis, G. H.; Hasted, J. B.; Buchanan, T. J. *J. Chem. Phys.* **1952**, *20*, 1452.
(47) Worley J. D.; Klotz I. M. *J. Chem. Phys.* **1966**, *45*, 2868.
(48) Walrafen G. E. *J. Chem. Phys.* **1964**, *40*, 3249; **1966**, *44*, 1546.
(49) Stillinger, F. H. *Science* **1980**, *209*, 4455.
(50) Eisenberg, D.; Kauzmann, W. *The Structure and Properties of Water*; Clarendon: Oxford, England, 1969.
(51) Luck, W. A. P. *Discuss. Faraday Soc.* **1967**, *43*, 115; 133.
(52) Mountain R. D. *J. Chem. Phys.* **1989**, *90*, 1866.
(53) Pimentel, G. C.; McClellan, A. L. *Annu. Rev. Phys. Chem.* **1971**, *22*, 347.

MA010804E